Survival of charged ρ condensation at high temperature and density*

Hao Liu(刘好)[1;1)] Lang Yu(余浪)[1;2)] Mei Huang(黄梅)[1,2;3)]

[1] Institute of High Energy Physics, Chinese Academy of Sciences, Beijing 100049, China
[2] Theoretical Physics Center for Science Facilities, Chinese Academy of Sciences, Beijing 100049, China

Abstract: The charged vector ρ mesons in the presence of external magnetic fields at finite temperature T and chemical potential μ have been investigated in the framework of the Nambu–Jona-Lasinio model. We compute the masses of charged ρ mesons numerically as a function of the magnetic field for different values of temperature and chemical potential. The self-energy of the ρ meson contains the quark-loop contribution, i.e. the leading order contribution in $1/N_c$ expansion. The charged ρ meson mass decreases with the magnetic field and drops to zero at a critical magnetic field eB_c, which indicates that the charged vector meson condensation, i.e. the electromagnetic superconductor can be induced above the critical magnetic field. Surprisingly, it is found that the charged ρ condensation can even survive at high temperature and density. At zero temperature, the critical magnetic field just increases slightly with the chemical potential, which indicates that charged ρ condensation might occur inside compact stars. At zero density, in the temperature range $0.2-0.5$ GeV, the critical magnetic field for charged ρ condensation is in the range of $0.2-0.6$ GeV^2, which indicates that a high temperature electromagnetic superconductor might be created at LHC.

Keywords: magnetic field, charged ρ condensation, temperature, chemical potential

PACS: 13.40.-f, 25.75.-q, 11.10.Wx **DOI:** 10.1088/1674-1137/40/2/023102

1 Introduction

Quantum chromodynamics (QCD) is widely accepted as the fundamental theory for strong interaction. Exploring QCD phase structure and properties of QCD matter in extreme conditions is one of the most important topics in high energy nuclear physics. Recently, it has become more and more attractive to study properties of QCD matter under strong magnetic fields. Strong magnetic fields could exist in various physical systems, e.g. the strength of magnetic fields can reach up to 10^{14} G in magnetars, and the magnitude of magnetic fields may be as high as 10^{18-23} G in the early universe. In particular, in the laboratory, a strong magnetic field with a strength of 10^{18-20} G (i.e. $eB\sim 0.1-1$ GeV^2) can be generated in the early stage of non-central heavy ion collisions [1, 2] at the Relativistic Heavy Ion Collider (RHIC) or the LHC. Therefore, heavy ion collisions offer a unique platform to probe properties of QCD vacuum and hot/dense quark matter under strong magnetic fields.

Magnetic fields can modify the spectrum of charged particles, and the energy levels of free charged particles in an external magnetic field parallel to z axis are given as $E^2_{n,s_z}(p_z)=p_z^2+(2n-2\text{sgn}(q)s_z+1)|qB|+m^2$, where the nonnegative integer n is the Landau level, s_z is the spin projection, and p_z is the particle's momentum in the direction of the magnetic field. Hence, $m^2_{\pi^\pm}(B)=m^2_{\pi^\pm}(B=0)+eB$ and $m^2_{\rho^\pm}(B)=m^2_{\rho^\pm}(B=0)-eB$ describe the minimal effective squared masses of charged π and charged ρ, respectively. As the magnetic field increases, the charged π mesons become heavier while the polarized charged ρ mesons become lighter. Chernodub first proposed that charged ρ meson can form a superconductor state when the magnetic field is stronger than the critical magnetic field $eB_c\approx m^2_{\rho^\pm}(B=0)\approx 0.6$ GeV^2 [3, 4]. This characterizes a quantum phase transition caused only by the magnetic field, which is a surprising result.

It is still under investigation whether there exists a vacuum superconductor. In Ref. [5], it was argued

Received 23 July 2015
* Supported by the NSFC (11275213, 11261130311) (CRC 110 by DFG and NSFC), CAS Key Project (KJCX2-EW-N01), and Youth Innovation Promotion Association of CAS. L.Yu is Partially Supported by China Postdoctoral Science Foundation (2014M550841)
1) E-mail: haoliu@mail.ihep.ac.cn
2) E-mail: yulang@mail.ihep.ac.cn
3) E-mail: huangm@mail.ihep.ac.cn

that the vacuum superconductor phase cannot appear due to the Vafa–Witten theorem. As pointed out in Ref. [6], the non-condensate results obtained in Ref. [5] are due to choosing the generating functional on the symmetric vacuum from the very beginning. In general, one should solve the real vacuum from the effective action with external source which should allow the non-symmetric vacuum solution. Therefore, the Vafa–Witten theorem would not forbid charged ρ meson condensation in an external magnetic field. More studies on charged ρ condensation have been done in different frameworks such as the Nambu–Jona-Lasinio (NJL) model [7, 8], lattice QCD [5, 9], the gauge/gravity correspondence [10, 11], the relativistic Hamiltonian technique [12], and the Dyson–Schwinger equations [13]. On one hand, it was observed that the masses of charged ρ mesons first decrease and then increase with the magnetic field, and cannot drop to zero, as shown by lattice calculations [5], Dyson–Schwinger equations [13] and by solving the meson spectra in a relativistic quark-antiquark system with the relativistic Hamiltonian technique in Ref. [12]. On the other hand, some other results showed that the charged ρ masses indeed decrease with magnetic field and become massless at a critical magnetic field as shown in the NJL model [4, 7, 8] and in the holographic QCD model [10].

Furthermore, for charged ρ condensation, the obtained results for the critical magnetic field are quite different in different calculations. For example, polarized $\rho^{\pm}$ condensation is expected to occur at the critical magnetic field $eB_{\rm c} \approx 1$ GeV^2 in lattice QCD [9], and $eB_{\rm c} \approx 1.08 m_\rho^2(B=0)$ is given in Ref. [10] in a holographic approach. Even in the framework of the NJL model, the results for the critical magnetic field differ a lot. The critical magnetic field $eB_{\rm c} > 1$ GeV^2 was obtained in Ref. [4] by ignoring the quark-loop contribution, and $eB_{\rm c} = 0.98 M_{\rm q}^2$ was given in Ref. [7], where $M_{\rm q}$ is the quark mass. In Ref. [8], we have obtained the critical magnetic field $eB_{\rm c} \approx 0.2$ GeV^2 in the NJL model by calculating the ρ meson polarization function to the leading order of $1/N_{\rm c}$ expansion.

By taking the quark propagator in the Ritus form as well as the Landau level representation, we have obtained the same results for the critical magnetic field $eB_{\rm c} \approx 0.2$ GeV^2, which is only 1/3 of the results from the point-particle calculation in Ref. [3]. Our results suggest that charged ρ condensation can be realized in nature much easier than that in Ref. [3]. In this work, we are going to study charged ρ mesons in a magnetic field at finite temperature and chemical potential in the framework of the NJL model, and investigate the temperature and density region for the survival of charged ρ condensation. This paper is organized as follows: In Sec. 2, we give a general description of the two-flavor NJL model including the effective four-quark interaction in the vector channel, and derive the vector meson mass under magnetic fields at finite temperature and chemical potential. We give numerical results and analysis in Sec. 3 and finally in Sec. 4 the discussion and conclusion is given.

2 Model and formalism

2.1 The two-flavor magnetized NJL model

In this paper, we investigate the properties of the charged ρ meson under magnetic fields with nonzero temperature T and chemical potential μ in the framework of the $SU(2)$ NJL model. The NJL model, seen as a low-energy approximation of QCD, is regarded as an effective theory to study the properties of mesons [14–19]. In our model, the Lagrangian density is given by

$$\mathcal{L} = \bar{\psi}({\rm i}\not{D} - \hat{m} + \mu\gamma^0)\psi + G_{\rm S}\left[(\bar{\psi}\psi)^2 + (\bar{\psi}{\rm i}\gamma^5\vec{\tau}\psi)^2\right] \\ -G_{\rm V}\left[(\bar{\psi}\gamma^\mu\tau^a\psi)^2 + (\bar{\psi}\gamma^\mu\gamma^5\tau^a\psi)^2\right] - \frac{1}{4}F_{\mu\nu}F^{\mu\nu}. \quad (1)$$

In the above equation, ψ corresponds to the quark field of two light flavors u and d, $\hat{m} = {\rm diag}(m_{\rm u}, m_{\rm d})$ is the current quark mass matrix of u and d quarks, $\tau^a = (I, \vec{\tau})$ with $\vec{\tau} = (\tau^1, \tau^2, \tau^3)$ corresponding to the isospin Pauli matrices, and $G_{\rm S}$ and $G_{\rm V}$ are the coupling constants with respect to the scalar (pseudoscalar) and the vector (axial-vector) channels, respectively. The covariant derivative, $D_\mu = \partial_\mu - {\rm i}q_{\rm f}A_\mu^{\rm ext}$, couples quarks to an external magnetic field $\boldsymbol{B} = (0,0,B)$ along the positive z direction via a background field, for example, $A_\mu^{\rm ext} = (0,0,Bx,0)$. $q_{\rm f} = (-1/3, 2/3)$ is defined as the electric charge of the quark field. The field strength tensor $F_{\mu\nu}$ is defined as usual by $F_{\mu\nu} = \partial_{[\mu}A_{\nu]}^{\rm ext}$, with $A_\mu^{\rm ext}$ fixed as above.

The semibosonized Lagrangian which is equivalent to the above Lagrangian is given by

$$\mathcal{L}_{\rm sb} = \bar{\psi}(x)\left({\rm i}\gamma^\mu D_\mu - \hat{m} + \mu\gamma^0\right)\psi(x) - \bar{\psi}\left(\sigma + {\rm i}\gamma_5\vec{\tau}\cdot\vec{\pi}\right)\psi \\ -\frac{(\sigma^2+\vec{\pi}^2)}{4G_{\rm S}} + \frac{(V_\mu^a V^{a\mu} + A_\mu^a A^{a\mu})}{4G_{\rm V}} - \frac{B^2}{2}, \quad (2)$$

where the Euler–Lagrange equation of motion for the auxiliary fields lead to the constraints

$$\sigma(x) = -2G_{\rm S} < \bar{\psi}(x)\psi(x) >, \quad (3)$$

$$\vec{\pi}(x) = -2G_{\rm S} < \bar{\psi}(x){\rm i}\gamma_5\vec{\tau}\psi(x) >, \quad (4)$$

$$V_\mu^a(x) = -2G_{\rm V} < \bar{\psi}(x)\gamma_\mu\tau^a\psi(x) >, \quad (5)$$

$$A_\mu^a(x) = -2G_{\rm V} < \bar{\psi}(x)\gamma_\mu\gamma^5\tau^a\psi(x) >. \quad (6)$$

The quarks obtain the dynamical masses by the quark-antiquark condensation, so the constituent quark mass M of u and d is defined by

$$M = m_0 - 2G_{\rm S} < \bar{\psi}\psi >, \quad (7)$$

where we assume $m_{\rm u}=m_{\rm d}=m_0$. To determine the dynamical quark mass, in other words, the σ condensation, we need to minimize the effective potential. The one-loop level effective potential of the model is given by

$$\varOmega=\frac{\sigma^2}{4G_{\rm S}}+\frac{B^2}{2}-3\sum_{q_{\rm f}\in\{\frac{2}{3},-\frac{1}{3}\}}\frac{|q_{\rm f}eB|}{\beta}\sum_{p=0}^{+\infty}\alpha_p\int_{-\infty}^{+\infty}\frac{{\rm d}p_3}{4\pi^2}\left\{\beta E_q+\ln\left(1+{\rm e}^{-\beta(E_q+\mu)}\right)+\ln\left(1+{\rm e}^{-\beta(E_q-\mu)}\right)\right\},\tag{8}$$

where $\beta=\dfrac{1}{T}$ and $\alpha_p=2-\delta_{p0}$ is the spin degeneracy factor.

In the NJL model, mesons are constructed by an infinite sum of quark-loop chains by using the random phase approximation. We calculate the ρ meson polarization function to the leading order of $1/N_{\rm c}$ expansion. The propagator of the ρ meson $D^{\mu\nu}_{ab}(q^2)$ can be obtained from the one quark loop polarization $\varPi_{\mu\nu,ab}(q^2)$ via the Dyson–Schwinger equation and takes the form of

$$[-{\rm i}D^{\mu\nu}_{ab}]=[-2{\rm i}G_{\rm V}\delta_{ab}g^{\mu\nu}]+\left[-2{\rm i}G_{\rm V}\delta_{ac}g^{\mu\lambda}\right][-{\rm i}\varPi_{\lambda\sigma,cd}][-{\rm i}D^{\sigma\nu}_{db}],\tag{9}$$

where a,b,c,d are isospin indices and μ, ν, λ, σ are Lorentz indices. The one-loop polarization $\varPi^{\mu\nu,ab}(q^2)$ is given by

$$\varPi^{\mu\nu,ab}(q^2)=-{\rm i}\int{\rm d}^4x\ {\rm e}^{{\rm i}q\cdot x}{\rm Tr}[\gamma^\mu\tau^a S_{\rm Q}(x,0)\gamma^\nu\tau^b\times S_{\rm Q}(0,x)].\tag{10}$$

Here, $S_{\rm Q}(x,y)$ is the Ritus fermion propagator [20, 21]

$$S_{\rm Q}(x,y)={\rm i}\sum_{p=0}^{\infty}\int\mathcal{D}\tilde{p}\ {\rm e}^{-{\rm i}\tilde{p}\cdot(x-y)}P_p(x_1)D^{-1}_{\rm Q}(\bar{p})\ P_p(y_1),\tag{11}$$

arising from the solution of the Dirac equation under a uniform magnetic field using the Ritus eigenfunction method. In Eq.(11), $\tilde{p}=(p_0,0,p_2,p_3)$, $\mathcal{D}\tilde{p}\equiv\dfrac{{\rm d}p_0{\rm d}p_2{\rm d}p_3}{(2\pi)^3}$, and $P_p(x_1)$ is given by

$$P_p(x_1)=\frac{1}{2}[f^{+s}_p(x_1)+\varPi_p f^{-s}_p(x_1)]+\frac{{\rm i}s_{\rm Q}}{2}[f^{+s}_p(x_1)-\varPi_p f^{-s}_p(x_1)]\gamma^1\gamma^2,\tag{12}$$

where, $\varPi_p\equiv 1–\delta_{p,0}$ considering the spin degeneracy in the LLL, $s_{\rm Q}\equiv{\rm sgn}(QeB)$. The functions $f^{\pm s}_p(x_1)$ are defined by

$$\begin{aligned}f^{+s}_p(x_1)&\equiv\phi_p\left(x_1-s_{\rm Q}p_2\ell_B^2\right),\qquad p=0,1,2,\cdots,\\ f^{-s}_p(x_1)&\equiv\phi_{p-1}\left(x_1-s_{\rm Q}p_2\ell_B^2\right),\qquad p=1,2,3,\cdots,\end{aligned}\tag{13}$$

where $\phi_p(x)$ is a function of Hermite polynomials $H_p(x)$ in the form

$$\phi_p(x)\equiv a_p\exp\left(-\frac{x^2}{2\ell_B^2}\right)H_p\left(\frac{x}{\ell_B}\right).\tag{14}$$

Here, $a_p\equiv(2^p p!\sqrt{\pi}\ell_B)^{-1/2}$ is the normalization factor and $\ell_B\equiv|QeB|^{-1/2}$ is the magnetic length. In Eq.(11), $D_{\rm Q}(\bar{p})=\gamma\cdot\bar{p}_{\rm Q}-M$ with the Ritus four momentum $\bar{p}=(p_0,0,-s_{\rm Q}\sqrt{2|QeB|p},p_3)$. Note that Q is a 2×2 matrix in the flavor space, so the functions $f^{\pm s}_p(x_1)$ are matrices in the flavor space.

Using the propagator in Eq.(11), the one quark loop polarization function $\varPi_{\mu\nu,ab}(q^2)$ is given by

$$\varPi^{\mu\nu,ab}(q^2)={\rm i}\sum_{p,k=0}^{\infty}\int\mathcal{D}\tilde{p}\ \mathcal{D}\tilde{k}\int{\rm d}^4x{\rm e}^{-{\rm i}(\tilde{p}-\tilde{k}-q)\cdot x}\times\varLambda^{\mu\nu,ab}_{pk}(\bar{p},\bar{k},x_1),\tag{15}$$

where

$$\varLambda^{\mu\nu,ab}_{pk}(\bar{p},\bar{k},x_1)={\rm Tr}\left[\gamma^\mu\tau^a P_p(x_1)D^{-1}_{\rm Q}(\bar{p})P_p(0)\gamma^\nu\tau^b\times K_k(0)D^{-1}_{\rm Q}(\bar{k})K_k(x_1)\right].\tag{16}$$

We can get the boundary conditions $q_i=p_i–k_i$ $(i=0,2,3)$ by integrating over x_0,x_2,x_3 and then over p_0,p_2,p_3 components in Eq.(15). So we get

$$\varPi^{\mu\nu,ab}(q^2)={\rm i}\sum_{p,k=0}^{\infty}\int\frac{{\rm d}k_0{\rm d}k_3}{(2\pi)^3}\int{\rm d}k_2{\rm d}x_1{\rm e}^{{\rm i}q_1x_1}\times\varLambda^{\mu\nu,ab}_{pk}(\bar{p},\bar{k},x_1)\big|_{b.c}.\tag{17}$$

In the above equation Eq.(17), the *b.c* is short for boundary conditions.

2.2 Charged ρ meson in a magnetic field at nonzero T and μ

In the rest frame of ρ, the Lorentz and flavor structure of the one quark loop polarization allows for the following decomposition

$$\varPi^{\mu\nu}_{ab}(q^2)=[\varPi^2_1(q^2)P^{\mu\nu}_1+\varPi^2_2(q^2)P^{\mu\nu}_2+\varPi^2_3(q^2)L^{\mu\nu}+\varPi^2_4(q^2)u^\mu u^\nu]\delta_{ab},\tag{18}$$

where $u^\mu=(1,0,0,0)$ is the 4-velocity in the rest frame. Here, we define the spin projection operators

$$P^{\mu\nu}_1=-\epsilon^\mu_2\epsilon^{\nu*}_2,\ (s_z=-1\ \text{for ρ}),\tag{19}$$

$$P^{\mu\nu}_2=-\epsilon^\mu_1\epsilon^{\nu*}_1,\ (s_z=1\ \text{for ρ}),\tag{20}$$

$$L^{\mu\nu}=-b^\mu b^\nu,\ (s_z=0\ \text{for ρ}),\tag{21}$$

where $b^\mu=(0,0,0,1)$ corresponds to the external magnetic field direction and ϵ^μ_1, ϵ^μ_2 are the right- and left-handed polarization vectors

$$\epsilon^\mu_1=\frac{1}{\sqrt{2}}(0,1,i,0),\tag{22}$$

$$\epsilon^\mu_2=\frac{1}{\sqrt{2}}(0,1,-i,0).\tag{23}$$

As a consequence, we can rewrite the propagator of ρ meson in Eq.(9) as

$$D_{ab}^{\mu\nu}(q^2)=[D_1(q^2)P_1^{\mu\nu}+D_2(q^2)P_2^{\mu\nu}+D_3(q^2)L^{\mu\nu}+D_4(q^2)u^\mu u^\nu]\delta_{ab}, \tag{24}$$

where

$$D_i(q^2)=\frac{2G_{\rm V}}{1+2G_{\rm V}\Pi_i^2}. \tag{25}$$

At last, we use the following gap equations to determine the masses of ρ meson with different spin projections

$$1+2G_{\rm V}\Pi_i^2=0. \tag{26}$$

In Eq.(16), the isospin Pauli matrices are $\tau^a=\tau^\pm$ and $\tau^b=\tau^\mp$ for charged $\rho^\pm$ meson, and $\tau^\pm=\frac{1}{\sqrt{2}}(\tau^1\pm {\rm i}\tau^2)$. In the rest frame of ρ meson, i.e., $q_\mu=(M_{\rho^\pm},\mathbf{0})$, the one quark loop polarization function takes the form of

$$\Pi_{\rho^\pm}^{\mu\nu}(q^2)={\rm i}\sum_{p,k=0}^{\infty}\int\frac{{\rm d}k_0{\rm d}k_3}{(2\pi)^3}\int {\rm d}k_2{\rm d}x_1\Lambda_{\rho^\pm,pk}^{\mu\nu}(\bar{p},\bar{k},x_1)\big|_{b.c}. \tag{27}$$

After calculating the $\Pi_{\rho^\pm}^{\mu\nu}(q^2)$ in the rest frame of ρ meson (the details are given in [8]), we can get the matrix as follows:

$$\Pi_{\rho^\pm}^{\mu\nu}=\begin{pmatrix}0&0&0&0\\0&\Pi^{11}&\Pi^{12}&0\\0&\Pi^{21}&\Pi^{22}&0\\0&0&0&\Pi^{33}\end{pmatrix}=\begin{pmatrix}0&0&0&0\\0&a&{\rm i}b&0\\0&-{\rm i}b&a&0\\0&0&0&c\end{pmatrix}. \tag{28}$$

Here, we define $\Pi^{11}=\Pi^{22}=a$, $\Pi^{12}=-\Pi^{21}={\rm i}b$ and $\Pi^{33}=c$. Note that the calculation in [8] was finished in the vacuum. However, in this paper, we are going to investigate the charged ρ condensation at finite temperature and density. Therefore, k_0 should be replaced by the Matsubara frequency summation, which is given in the Appendix . The matrix elements $\Pi^{11}=\Pi^{22}$, $\Pi^{12}=-\Pi^{21}$ and Π^{33} for ρ^+ at finite temperature are given as follows:

$$\begin{aligned}\Pi^{11}=\Pi^{22}&=24\sum_{p,k=0}^{\infty}\int\frac{{\rm d}k_3}{(2\pi)^2}\int{\rm d}k_2{\rm d}x_1\\&\quad\times\{\mathcal{A}A^+\alpha^++\mathcal{B}A^-\alpha^-\},\\\Pi^{12}=-\Pi^{21}&=24\sum_{p,k=0}^{\infty}\int\frac{{\rm d}k_3}{(2\pi)^2}\int{\rm d}k_2{\rm d}x_1\\&\quad\times\{\mathcal{B}(-{\rm i}s_uA^-\alpha^+)+\mathcal{A}(-{\rm i}s_uA^+\alpha^-)\},\\\Pi^{33}&=24\sum_{p,k=0}^{\infty}\int\frac{{\rm d}k_3}{(2\pi)^2}\int{\rm d}k_2{\rm d}x_1\\&\quad\times\{\mathcal{D}B^+\beta^++\mathcal{C}B^-\beta^-\}.\end{aligned} \tag{29}$$

The definitions of $\mathcal{A}$, $\mathcal{B}$, $\mathcal{C}$ and $\mathcal{D}$ are in the Appendix , and $A^\pm$, $\alpha^\pm$, $B^\pm$ and $\beta^\pm$ are represented as follows:

$$\begin{aligned}A^\pm&=\frac{1}{2}\left[f_p^{+s_u}(x_1)f_k^{+s_d}(x_1)\pm\Pi_p\Pi_kf_p^{-s_u}(x_1)f_k^{-s_d}(x_1)\right],\\\alpha^\pm&=\frac{1}{2}\left[f_p^{+s_u}(0)f_k^{+s_d}(0)\pm\Pi_p\Pi_kf_p^{-s_u}(0)f_k^{-s_d}(0)\right],\\B^\pm&=\frac{1}{2}[\Pi_pf_k^{+s_d}(x_1)f_p^{-s_u}(x_1)\pm\Pi_kf_p^{+s_u}(x_1)f_k^{-s_d}(x_1)],\\\beta^\pm&=\frac{1}{2}[\Pi_pf_k^{+s_d}(0)f_p^{-s_u}(0)\pm\Pi_kf_p^{+s_u}(0)f_k^{-s_d}(0)].\end{aligned} \tag{30}$$

where $\{s_u,s_d\}=\{{\rm sgn}(q_ueB),{\rm sgn}(q_deB)\}$ and $\{q_u,q_d\}=\{2/3,-1/3\}$.

Combining the expression in Eq.(18) and the matrix in Eq.(28), we can easily find the relation for charged $\rho^\pm$ meson

$$\begin{aligned}\Pi_1^2&=-(a+b),\\\Pi_2^2&=b-a,\\\Pi_3^2&=-c.\end{aligned} \tag{31}$$

As it has been discussed in [22], Π_4^2 should be zero in the rest frame of ρ mesons, guaranteed by the Ward identity.

3 Numerical results and discussions

3.1 Parameters

For numerical calculations, we use the soft cut-off functions in Refs.[8, 24]

$$f_\Lambda=\sqrt{\frac{\Lambda^{10}}{\Lambda^{10}+\boldsymbol{k}^{2*5}}}, \tag{32}$$

$$f_{\Lambda,eB}^k=\sqrt{\frac{\Lambda^{10}}{\Lambda^{10}+(k_3^2+2|QeB|k)^5}}, \tag{33}$$

for zero and nonzero magnetic fields, respectively. At finite magnetic field, we sum up to 20 Landau levels, and the results are saturated. Following Refs.[8, 23], the parameters of our model, namely the coupling constants $G_{\rm S}$ and $G_{\rm V}$, the current quark mass m_0, and the three-momentum cut-off Λ, are determined by reproducing the pion decay constant f_π, the quark mass M, the mass of π, and the mass of ρ in the vacuum. We obtain $\Lambda=582$ MeV, $G_{\rm S}\Lambda^2=2.388$, $G_{\rm V}\Lambda^2=1.73$, and $m_0=5$ MeV by choosing $f_\pi=95$ MeV, $m_\pi=140$ MeV, $M_\rho=768$ MeV, the vacuum quark mass $M=458$ MeV.

3.2 Numerical results for charged $\rho^\pm$ and discussions

In our numerical calculations, we first solve the gap equation Eq.(7) to obtain the quark constitute mass M, and then solve the gap equations of Eq.(26) for charged vector mesons.

Figure 1 shows the quark mass dependence of magnetic field eB at several fixed temperatures T and chemical potentials μ, and Fig. 2 describes the quark mass dependence of the temperature T at $\mu=0$ for several different magnetic fields eB. It is noticed that in the current model, there is no mechanism for inverse magnetic catalysis around the critical temperature. Therefore, Fig. 1 and Fig. 2 only show magnetic catalysis behavior of the quark mass.

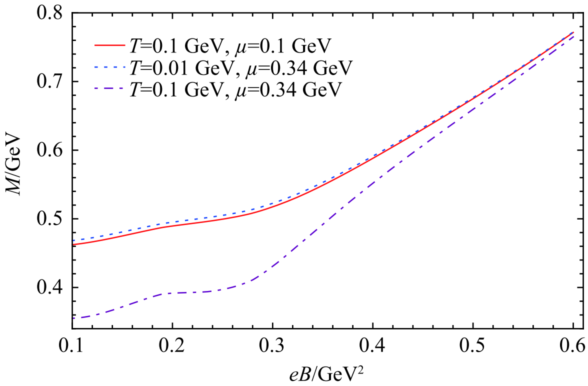

Fig. 1. (color online) The constituent quark mass M as a function of magnetic field eB with different temperatures T and chemical potentials μ.

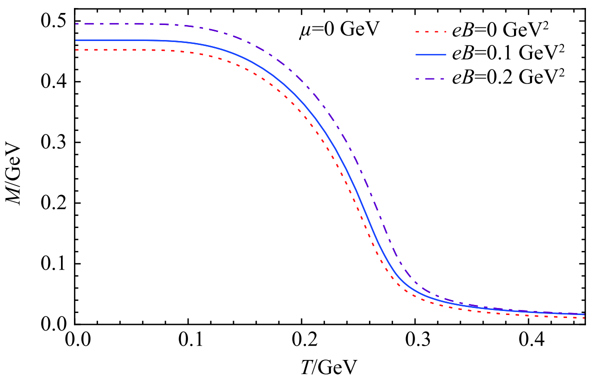

Fig. 2. (color online) The constituent quark mass M as a function of the temperature T with different magnetic field eB and zero chemical potential $\mu=0$.

In Ref. [8], we have observed that there is possible condensation of charged $\rho^{+}(\rho^{-})$ with $s_z=+1(s_z=-1)$ in the vacuum when the magnetic field is stronger than the critical magnetic field $eB_{\rm c}\approx 0.2$ GeV^2. The main goal of this work is to investigate the melting of the charged ρ condensation at finite temperature and chemical potential.

Figure 3 shows the mass of charged $\rho^{\pm}$ as the function of the magnetic field eB at zero temperature for different chemical potentials. It is observed from Fig. 3 that at zero temperature, when μ is smaller than the vacuum constituent quark mass $M_q^0=458$ MeV, the behavior of magnetic field dependence of the charged $\rho^{\pm}$ mass almost does not change for different chemical potentials, and the critical magnetic field remains as $eB_{\rm c}=0.2$ GeV^2. This indicates that charged ρ condensation can survive at high baryon density and might occur inside compact stars.

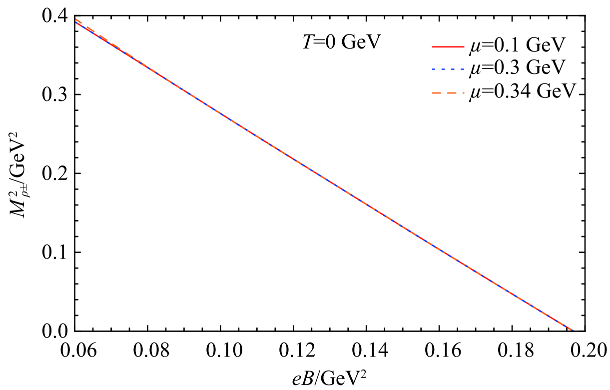

Fig. 3. (color online) The mass of charged $\rho^{+}(\rho^{-})$ with $s_z=+1(s_z=-1)$ in a magnetic field with fixed $T=0$ MeV with different chemical potentials μ.

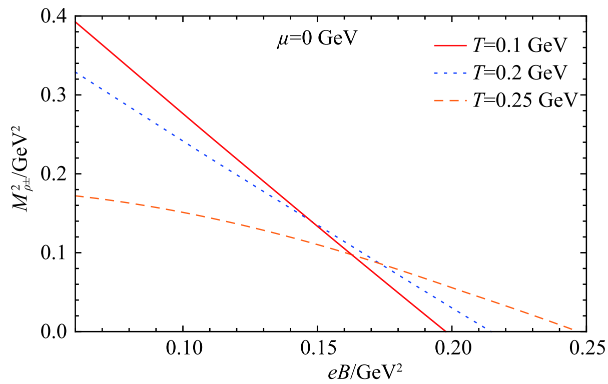

Fig. 4. (color online) The mass of charged $\rho^{+}(\rho^{-})$ with $s_z=+1(s_z=-1)$ in a magnetic field with fixed $\mu=0$ MeV and different temperatures T.

Figure 4 shows the mass of charged $\rho^{\pm}$ as a function of the magnetic field eB at zero chemical potential for different temperatures. It is seen that for different temperatures, the charged $\rho^{\pm}$ mass decreases with the magnetic field and drops to zero at the critical magnetic field. With the increase of temperature, the critical magnetic field also increases. This indicates that charged ρ condensation can survive even at high temperatures.

Lastly, in Fig. 5, we show the critical magnetic field $eB_{\rm c}$ as a function of the temperature for $\mu=0,0.3,0.46$ GeV, respectively. It can be known that when the temperature increases, the critical magnetic field increases. Furthermore, it is seen that the critical magnetic field increases with the chemical potential at fixed temperature. It is worth mentioning that at zero chemical potential, when the temperature is below $T=250$ MeV, which is almost the critical temperature for the chiral phase transition, we can find that the critical magnetic field does not change so much compared with its value at zero temperature. However, when the temperature is higher than $T = 250$ MeV, it is found that the critical magnetic field increases linearly with the temperature, and in the temperature range $200-500$ MeV, the critical magnetic field for charged ρ condensation is in the range of $0.2-0.6$ GeV^2, which is just located inside the range of the magnetic field generated in the non-central heavy ion collisions of the LHC. This means that a high temperature superconductor could be produced at LHC.

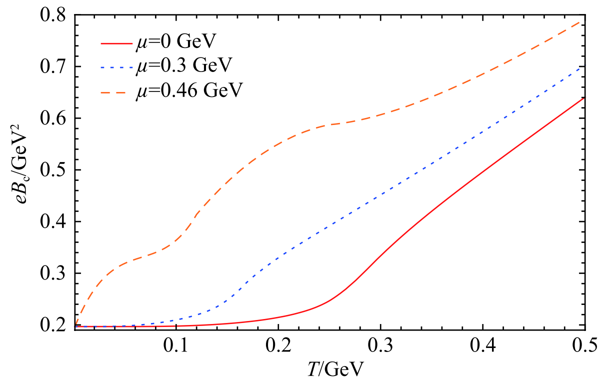

Fig. 5. (color online) The critical magnetic field eB_c as a function of temperature T with different chemical potential μ .

4 Conclusions

We have investigated the mass behavior of charged ρ mesons in the background without ρ condensation under external magnetic field at finite temperature and density by using the NJL model. When the charged ρ meson mass drops to zero or becomes negative, it indicates that this background is not stable, and a new charged ρ condensation would be developed. The mesons are constructed as in the vacuum by summing up infinite quark-loop chains using the random phase approximation. In this paper, we calculate the ρ meson polarization tensor to the leading order of $1/N_c$ expansion, i.e. the one quark loop. In this process, the constituent quark mass is solved self-consistently with magnetic field at finite temperature and density. It is noticed that in our current framework, there is no inverse magnetic catalysis mechanism, so the quark mass increases with magnetic field and only shows the magnetic catalysis effect.

The mass of charged ρ meson depending on the magnetic field is calculated at finite temperature and density. It is found that at fixed temperature and density, the polarized charged ρ meson becomes lighter with the increase of magnetic fields and becomes massless at the critical magnetic field eB_c, which indicates that charged ρ meson condensation would appear when the strength of the magnetic field is greater than eB_c. Moreover, it is observed that the critical magnetic field eB_c increases with both the temperature and density. Particularly, at zero density, our results show that in the temperature region 200 MeV $< T <$ 500 MeV, the critical magnetic field eB_c is in the range of $0.2-0.6$ GeV^2, which indicates that the high temperature superconductor could be created in the early stage of the LHC.

However, we have to mention that in our current framework, there is no inverse magnetic catalysis for the quark mass. In the next step, we will investigate how the inverse magnetic catalysis [26] will affect our results on charge ρ condensation, especially at high temperatures.

We thank J.F. Liao and I. Shovkovy for valuable discussions.

Appendix A

Integrals of k_0

We introduce the notations of the integrals of k_0 for ρ^+ meson as follows:

$$\mathcal{A}=\mathrm{i}\int\frac{\mathrm{d}k_0}{2\pi}\frac{\bar{p}_{(u)}\cdot\bar{k}_{(d)}-M^2}{(p_0^2-\omega_{u,p}^2)(k_0^2-\omega_{d,k}^2)}=\frac{1}{2}(\mathrm{i}I_1+\mathrm{i}I_1')-\left[\frac{1}{2}\left(M_{\rho^+}^2-\bar{p}_{(2,u)}^2-\bar{k}_{(2,d)}^2\right)+\bar{p}_{(2,u)}\bar{k}_{(2,d)}\right]\mathrm{i}I_2, \quad \text{(A1)}$$

$$\mathcal{B}=\mathrm{i}\int\frac{\mathrm{d}k_0}{2\pi}\frac{\bar{p}_{(u)}\cdot\bar{k}_{(d)}-M^2+2\bar{p}_{(2,u)}\bar{k}_{(2,d)}}{(p_0^2-\omega_{u,p}^2)(k_0^2-\omega_{d,k}^2)}=\frac{1}{2}(\mathrm{i}I_1+\mathrm{i}I_1')-\left[\frac{1}{2}\left(M_{\rho^+}^2-\bar{p}_{(2,u)}^2-\bar{k}_{(2,d)}^2\right)-\bar{p}_{(2,u)}\bar{k}_{(2,d)}\right]\mathrm{i}I_2, \quad \text{(A2)}$$

$$\mathcal{C}=\mathrm{i}\int\frac{\mathrm{d}k_0}{2\pi}\frac{p_0k_0+\bar{p}_{(2,u)}\bar{k}_{(2,d)}+k_3^2-M^2}{(p_0^2-\omega_{u,p}^2)(k_0^2-\omega_{d,k}^2)}=\frac{1}{2}(\mathrm{i}I_1+\mathrm{i}I_1')+\left[2k_3^2-\frac{1}{2}\left(M_{\rho^+}^2-\bar{p}_{(2,u)}^2-\bar{k}_{(2,d)}^2\right)+\bar{p}_{(2,u)}\bar{k}_{(2,d)}\right]\mathrm{i}I_2, \quad \text{(A3)}$$

$$\mathcal{D}=\mathrm{i}\int\frac{\mathrm{d}k_0}{2\pi}\frac{p_0k_0-\bar{p}_{(2,u)}\bar{k}_{(2,d)}+k_3^2-M^2}{(p_0^2-\omega_{u,p}^2)(k_0^2-\omega_{d,k}^2)}=\frac{1}{2}(\mathrm{i}I_1+\mathrm{i}I_1')+\left[2k_3^2-\frac{1}{2}\left(M_{\rho^+}^2-\bar{p}_{(2,u)}^2-\bar{k}_{(2,d)}^2\right)-\bar{p}_{(2,u)}\bar{k}_{(2,d)}\right]\mathrm{i}I_2. \quad \text{(A4)}$$

Here, $\omega_{u,p}^2=2|q_ueB|p+p_3^2+M^2$, $\bar{p}_{(2,u)}=-s_u\sqrt{2|q_ueB|p}$ and $\bar{p}_{(u)}=(p_0,0,-s_u\sqrt{2|q_ueB|p},p_3)$, We use a similar definition for $\bar{k}_{(d)}$, $\bar{k}_{(2,d)}$, $\omega_{d,k}$. Moreover, I_1, I_1' and I_2 are given by:

$$I_1=\int\frac{\mathrm{d}k_0}{2\pi}\frac{1}{k_0^2-\omega_{u,p}^2}, \tag{A5}$$

$$I_1'=\int\frac{\mathrm{d}k_0}{2\pi}\frac{1}{k_0^2-\omega_{d,k}^2}, \tag{A6}$$

$$I_2=\int\frac{\mathrm{d}k_0}{2\pi}\frac{1}{((k_0+q_0)^2-\omega_{u,p}^2)(k_0^2-\omega_{d,k}^2)}. \tag{A7}$$

As in Ref. [25], we replace the integration over k_0 by Matsubara summation according to the prescription $\int\frac{\mathrm{d}k_0}{2\pi}(\cdots)\rightarrow \mathrm{i}T\sum_{m=-\infty}^{\infty}(\cdots)$ and obtain

$$\mathrm{i}I_1=-\left(\frac{n_\mathrm{f}(\omega_{u,p}-\mu)+n_\mathrm{f}(\omega_{u,p}+\mu)-1}{2\omega_{u,p}}\right), \tag{A8}$$

$$\mathrm{i}I_1'=-\left(\frac{n_\mathrm{f}(\omega_{d,k}-\mu)+n_\mathrm{f}(\omega_{d,k}+\mu)-1}{2\omega_{d,k}}\right), \tag{A9}$$

$$\begin{aligned}\mathrm{i}I_2=-\Bigg[&\frac{n_\mathrm{f}(\omega_{d,k}-\mu)}{2\omega_{d,k}}\frac{1}{(\omega_{d,k}+M_{\rho^+})^2-\omega_{u,p}^2}\\&-\frac{n_\mathrm{f}(-\omega_{d,k}-\mu)}{2\omega_{d,k}}\frac{1}{(-\omega_{d,k}+M_{\rho^+})^2-\omega_{u,p}^2}\\&+\frac{n_\mathrm{f}(\omega_{u,p}-\mu)}{2\omega_{u,p}}\frac{1}{(-M_{\rho^+}+\omega_{u,p})^2-\omega_{d,k}^2}\\&-\frac{n_\mathrm{f}(-\omega_{u,p}-\mu)}{2\omega_{u,p}}\frac{1}{(-M_{\rho^+}-\omega_{u,p})^2-\omega_{d,k}^2}\Bigg],\end{aligned} \tag{A10}$$

with

$$n_\mathrm{f}(x)=\frac{1}{1+\mathrm{e}^{\frac{x}{T}}}. \tag{A11}$$

Here, the notations are only for ρ^+ meson, and similar ones can be used for ρ^- meson.

References

1 V. Skokov, A. Y. Illarionov and V. Toneev, Int. J. Mod. Phys. A, **24**: 5925 (2009)
2 W. -T. Deng and X. -G. Huang, Phys. Rev. C, **85**: 044907 (2012)
3 M. N. Chernodub, Phys. Rev. D, **82**: 085011 (2010); [arXiv:1008.1055 [hep-ph]]
4 M. N. Chernodub, Phys. Rev. Lett., **106**: 142003 (2011); [arXiv:1101.0117 [hep-ph]]
5 Y. Hidaka and A. Yamamoto, Phys. Rev. D, **87** (9): 094502 (2013); [arXiv:1209.0007 [hep-ph]]
6 C. Li and Q. Wang, Phys. Lett. B, **721**: 141 (2013); [arXiv:1301.7009 [hep-th]]
7 M. Frasca, JHEP, **1311**: 099 (2013); [arXiv:1309.3966 [hep-ph]]
8 H. Liu, L. Yu and M. Huang, Phys. Rev. D, **91**: (1): 014017 (2015); [arXiv:1408.1318 [hep-ph]]
9 O. Larina, E. Luschevskaya, O. Kochetkov and O. V. Teryaev, PoS LATTICE, **2014**: 120 (2014); [arXiv:1411.0730 [hep-lat]]
10 N. Callebaut, D. Dudal and H. Verschelde, PoS FACESQCD , 046 (2010); [arXiv:1102.3103 [hep-ph]]
11 M. Ammon, J. Erdmenger, P. Kerner and M. Strydom, Phys. Lett. B, **706**: 94 (2011); [arXiv:1106.4551 [hep-th]]
12 M. A. Andreichikov, B. O. Kerbikov, V. D. Orlovsky and Y. A. Simonov, Phys. Rev. D, **87**: (9): 094029 (2013); [arXiv:1304.2533 [hep-ph]]
13 Kunlun Wang, *QCD phase transition and properties of phases with Dyson-Schwinger equations*, Ph.D. Thesis (Beijing: Peking University, 2013) (in Chinese)
14 Y. Nambu and G. Jona-Lasinio, Phys. Rev., **122**: 345 (1961)
15 Y. Nambu and G. Jona-Lasinio, Phys. Rev., **124**: 246 (1961)
16 S. Klimt, M. F. M. Lutz, U. Vogl and W. Weise, Nucl. Phys. A, **516**: 429 (1990)
17 U. Vogl and W. Weise, Prog. Part. Nucl. Phys., **27**: 195 (1991)
18 S. P. Klevansky, Rev. Mod. Phys., **64**: 649 (1992)
19 T. Hatsuda and T. Kunihiro, Phys. Rept., **247**: 221 (1994); [hep-ph/9401310]
20 S. Fayazbakhsh, S. Sadeghian and N. Sadooghi, Phys. Rev. D, **86**: 085042 (2012); [arXiv:1206.6051 [hep-ph]]
21 K. Fukushima, D. E. Kharzeev and H. J. Warringa, Nucl. Phys. A, **836**: 311 (2010); [arXiv:0912.2961 [hep-ph]]
22 A. K. Das and M. B. Hott, Mod. Phys. Lett. A, **9**: 3383 (1994); [hep-ph/9406426]
23 Y. B. He, J. Hufner, S. P. Klevansky and P. Rehberg, Nucl. Phys. A, **630**: 719 (1998); [nucl-th/9712051]
24 M. Frasca and M. Ruggieri, Phys. Rev. D, **83**: 094024 (2011); [arXiv:1103.1194 [hep-ph]]
25 P. Rehberg and S. P. Klevansky, Annals Phys., **252**: 422 (1996); [hep-ph/9510221]
26 J. Chao, P. Chu and M. Huang, Phys. Rev. D, **88**: 054009 (2013); L. Yu, H. Liu and M. Huang, Phys. Rev. D, **90**: (7): 074009 (2014); L. Yu, J. Van Doorsselaere and M. Huang, Phys. Rev. D, **91**: (7): 074011 (2015)